5.12 ANTARCTIC CLOUDS AND CLIMATE IN THE NCAR CLIMATE MODELS

Keith M. Hines[1], David H. Bromwich[1,2], Michael J. Iacono[3], and Philip J. Rasch[4]

[1]Polar Meteorology Group, Byrd Polar Research Center,
The Ohio State University, Columbus, Ohio

[2]Atmospheric Science Program, Department of Geography
The Ohio State University, Columbus, Ohio

[3]Atmospheric and Environmental Research, Inc., Lexington, MA

[4]National Center for Atmospheric Research, Boulder, Colorado

1. INTRODUCTION

The largest variance between the results of global climate models is found in the polar regions (e.g., Gates et al. 1996). Cloud radiative effects contribute to the difficulty of modeling the polar regions, as phenomena such as clear-sky precipitation and Arctic haze must be accounted for. Additional complications include extremely low surface temperatures and atmospheric moisture contents. Cloud emissivities are frequently much less than 1 (Lubin and Harper 1996; Randall et al. 1998). Near surface air is often saturated or supersaturated with respect to ice (Anderson 1993). Furthermore, the radiative flux is concentrated in different parts of the infrared spectrum than in warmer, wetter climates (Curry et al. 1996). Many common modeling parameterizations are designed for other environments and may not work well in polar regions (Pinto and Curry 1997; Randall et al. 1998). Fortunately, several recent projects have generated knowledge about clouds and radiative processes and their interactions in the Arctic. Now we must turn our attention to the Antarctic region. While water clouds are often present in the Arctic, clouds over interior Antarctica consist primarily of ice crystals (Morley et al. 1989). Furthermore, concentrations of condensation nuclei can be extremely low (Austin Hogan, personal communication, 2001). Modeling studies show that the simulated high southern latitude climate is highly sensitive to the radiation parameterization (Shibata and Chiba 1990; Lubin et al. 1998).

Simulations with previous generations of the National Center for Atmospheric Research (NCAR) climate models have demonstrated the difficulties representing the hydrologic cycle and radiative effects for the polar regions, especially Antarctica (Tzeng et al. 1993, 1994). Despite many improvements over the earlier Community Climate Model version 1 (CCM1), the NCAR CCM2 included deficiencies still significantly overestimated summertime cloud cover leading to a cold bias and shortwave deficit over Antarctica (Tzeng et al. 1994). During the late 1990s, CCM3 became the state-of-the-art atmospheric climate model at NCAR. Briegleb and Bromwich (1998a,b) examine the polar climate and radiation balance simulated by this enhanced model. Overall, They find the polar climate of CCM3 is an incremental improvement over that simulated by CCM2. Biases, however, still remain in the simulated polar radiation budget despite improvements in the global radiation fields (Briegleb and Bromwich 1998a). There is a summer deficit of absorbed shortwave of about 20 W m^{-2} for both polar regions, as the polar clouds are apparently too reflective. Furthermore, there is a deficit of at least 10 W m^{-2} in the downward clear-sky longwave radiation during the South Pole winter. Briegleb and Bromwich (1998a,b) suggest the causes of remaining deficiencies in the NCAR CCM3 include the following: (1) inadequate cloud cover and optical property representation, (2) inadequate surface albedo over sea ice and the Antarctic plateau, (3) systematic deficit in surface downward longwave radiation, (4) inadequate representation of the sea ice/atmosphere heat exchange resulting from the lack of both fractional sea ice coverage and variability of sea ice thickness, (5) limitations due to the T42 horizontal resolution, and (6) biases in the influence from the tropics and mid-latitudes. Here, we will consider points (1)-(3).

While Briegleb and Bromwich (1998a) report on the status of CCM3's polar radiation simulation, we now expand the evaluation to include new parameterizations and the most recent versions of the NCAR climate models. As there has been considerable focus recently on climate modeling in the Arctic, we choose to concentrate here on the Antarctic region. We examine how simulated climate responds to changes in polar cloud and radiation parameterizations, and how the simulated climate can be improved.

* *Corresponding author address:* Keith M. Hines, Polar Meteorology Group, Byrd Polar Research Center, The Ohio State University, 1090 Carmack Road, Columbus, OH 43210-1002.

2. NCAR CLIMATE MODELS

Several versions of the cloud and radiation parameterizations for the NCAR CCM3 are evaluated. Additionally, atmospheric output is evaluated for two benchmark simulations with standard versions of the new NCAR atmospheric model Community Atmosphere Model version 2 (CAM2) and the new NCAR coupled Community Climate System Model version 2 (CCSM2). The model CCM3, with T42 resolution and 18 levels in the vertical has refinements in the cloud parameterization over that of the earlier CCM2 (Kiehl et al. 1998). The diagnostic parameterizations for cloud fraction in standard CCM3, nearly identical to those of CCM2, are based upon improvements to the model of Slingo (1987). Cloud fraction is determined from the relative humidity, with vertical velocity, static stability and convective mass flux as additional inputs. Clouds can exist at all tropospheric levels above the surface layer. The optical properties of liquid water droplets are also parameterized the same way in both CCM2 and CCM3, based on the model of Slingo (1989). The major refinements to CCM3 involve the allowance for ice clouds as well as water clouds, and the difference in cloud particle sizes over land versus water. Between -10°C and -30°C, the fraction of total cloud water that is ice is specified to increase linearly from 0 to 1. The optical properties of ice particles are taken from Ebert and Curry (1992). The vertical distribution of cloud water is prescribed based upon the vertically-integrated water vapor. The model also incorporates the NCAR Land Surface Model (LSM, Bonan 1998).

The NCAR CCSM2 includes CAM2 for the atmospheric component, along with prognostic sea ice, land, and ocean components. The results of the two simulations will differ as the benchmark CAM2 simulation has prescribed climatological surface boundary conditions, while the CCSM2 simulation has simulated surface conditions that include interannual variability. The CAM2 has a horizontal resolution of T42 and 26 levels in the vertical. The difference in vertical resolution between CCM3 and CAM2 is primarily near the tropopause. The revised NCAR climate models have a new Community Land Model 2.0 and many other new features. Furthermore, the atmospheric model CAM2 now includes the Collins (2001) scheme to allow a greater variety of cloud overlap assumptions, new water vapor absorptivity and emissivity (Collins et al. 2002), improved representations of ozone and topography, and evaporation of precipitation.

The CCM3 simulations include two standard benchmark simulations performed at NCAR: A 14-year simulation, which we shall refer to as AMIP SST, which includes the period of the Atmospheric Model Intercomparison Project (AMIP) beginning in 1979, and 10 years of a simulation with climatological boundary conditions recycling every year, which we shall refer to as CLIMATE SST. In addition to the benchmark simulations with a standard version of CCM3, we also consider a CCM3 simulation, which we shall refer to as PREDICTED CLOUD WATER, with the standard global scheme for diagnostic cloud water and ice replaced with the more sophisticated predictive scheme of Rasch and Kristjansson (1998). With this scheme, clouds consist of ice particles for temperatures below -20°C, liquid drops for temperatures above 0°C, and are mixed phase for temperatures between -20°C and 0°C. The prognostic scheme was anticipated to provide a more realistic depiction of Antarctic clouds. Rasch and Kristjansson (1998) found the largest sensitivity to the change in cloud scheme for the Arctic during winter and the Antarctic for all seasons. The simulated seasonal cycle of cloud amount in the Arctic was improved. The simulation PREDICTED CLOUD WATER is for 14 years over the same time period as AMIP SST.

Also, Atmospheric and Environmental Research, Inc. has provided a version of the Rapid Radiative Transfer Model (RRTM, Mlawer et al. 1997; Iacono et al. 2000) longwave radiation code that can be included in CCM3. For clear skies, this radiation code yields larger downwelling longwave fluxes for polar atmospheric conditions than the standard version of the CCM3 radiation code. Column radiation calculations with RRTM show that it eliminates the polar clear-sky longwave bias found in many atmospheric climate models (Von Walden, personal communication 1999/2000). Therefore, we include in the model comparison a 10-year simulation referred to as RRTM performed by Atmospheric and Environmental Research, Inc. of the AMIP period.

To seek improved climate simulations, both the prognostic cloud particulate scheme of Rasch and Kristjansson (1998) and the Rapid Radiative Transfer Model (RRTM, Iacono et al. 2000) developed by Atmospheric and Environmental Research (Inc.) are implemented in CCM3, version 3.6. A 15-year simulation with climatological boundary conditions is performed. We refer to this new simulation as PCW+RRTM. Results are compared to the other CCM3 simulations. Some of the simulations have annually-varying boundary conditions for fields such as sea surface temperature. It was found, however, that the multi-year average fields for clouds and radiation are very similar for the CLIMATE SST and AMIP SST. Therefore, the differing boundary conditions do not appear to have a first-order effect on the simulations. For simplicity, only the results of CLIMATE SST are shown in the analysis that follows.

3. HIGH SOUTHERN LATITUDE TEMPERATURE

The CCM3 results show a high sensitivity to the clouds and radiation parameterizations over Antarctica. Figure 1 shows the monthly surface temperature at the South Pole and the winter (June, July and August) and summer (December, January and February) values as a function of latitude for several simulations. North of the pack ice surrounding Antarctica, CCM3 surface temperature is specified and not sensitive to the changes in parameterization (Figs. 1a and 1b). The

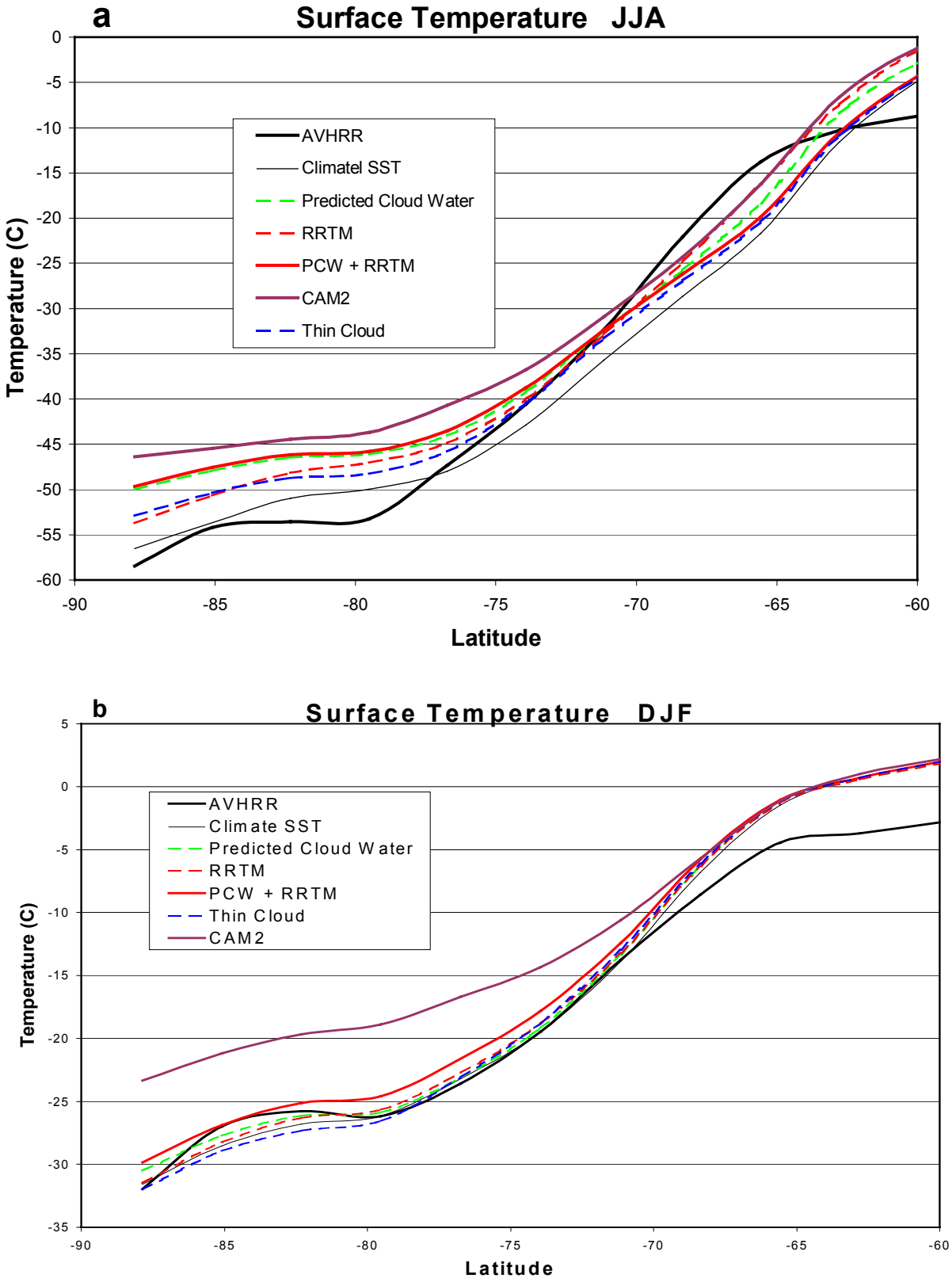

Figure 1. Surface temperature (ºC) from observations, satellite retrievals, and CCM3 and CAM2 model runs. Mean 3-month values versus latitude are shown for (a) winter (June, July and August) and (b) summer (December, January and February) and (c) monthly values at the South Pole versus time.

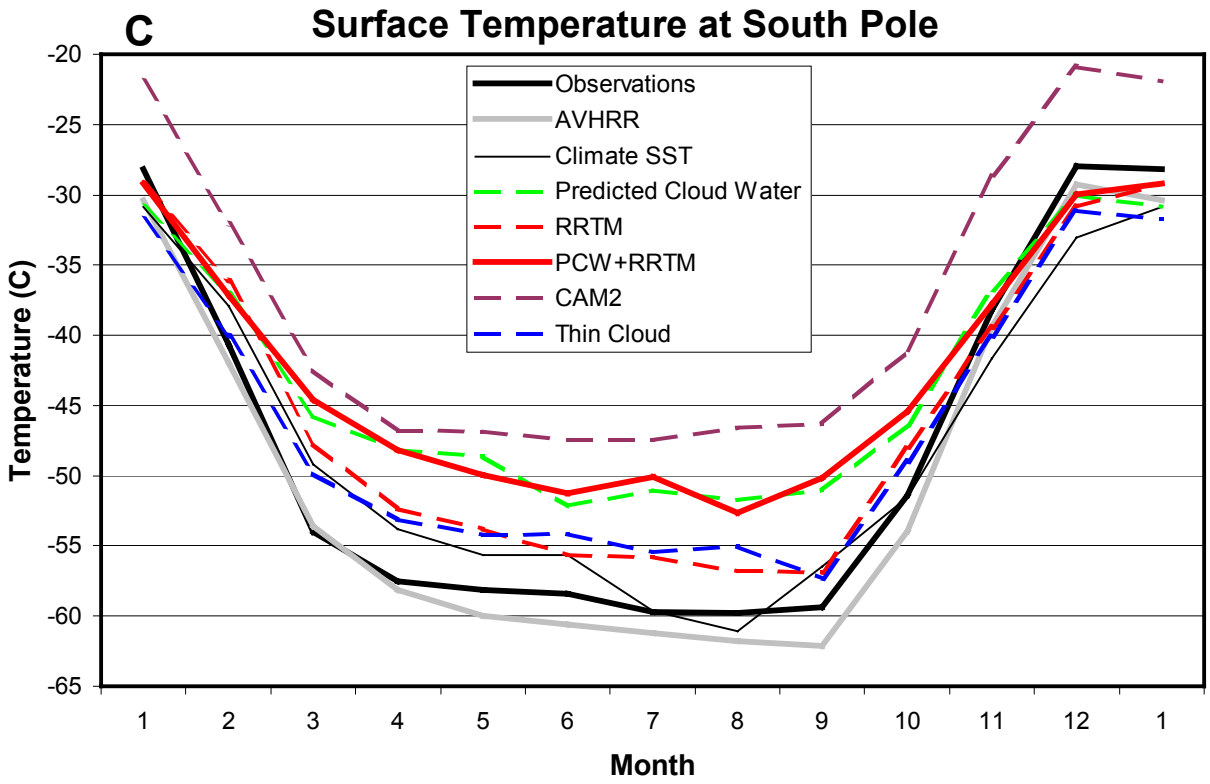

Figure 1. Surface temperature (ºC) from observations, satellite retrievals, and CCM3 and CAM2 model runs. Mean 3-month values versus latitude are shown for (a) winter (June, July and August) and (b) summer (December, January, and February) and (c) monthly values at the South Pole versus time.

latitudes of largest winter sensitivity are south of 75°S, indicating that the greatest sensitivity is over interior Antarctica. Therefore, we will focus on the interior of Antarctica. The observations in Fig. 1c show the 1957-2002 monthly-average surface air observations at Amundsen-Scott station (90°S) from the Reference Antarctic Data for Environmental Research (READER) dataset compiled by the Scientific Committee on Antarctic Research. Estimated surface temperature for 1982-1999 from the Advanced Very High Resolution Radiometer (AVHRR) Polar Pathfinder (Key 2001) is also shown. Comparison of the two shows that the AVHRR-derived surface temperature provides a reasonable estimate of the observed value (Fig. 1c). The AVHRR values are about 2°C colder than the observed temperature during winter, perhaps due to the temperature difference between the near-surface air and the typically colder snow surface. The surface temperatures for simulations with the standard version of CCM3, CLIMATE SST and AMIP SST, with climatological and AMIP sea surface temperatures, respectively, are very similar. Therefore, only the results for CLIMATE SST are shown.

Except for September, the standard version of CCM3 shows a reasonable surface temperature for late winter and spring. The early onset of winter cold temperatures beginning about April, however, is not well captured by CCM3. During the brief summer at South Pole, when shortwave radiation is an important component of the surface energy balance, the standard version of CCM3 is up to 5°C too cold. The simulation with the RRTM radiation code is about 5°C warmer than observations during winter and slightly colder than observations during summer. The warmer surface temperatures in RRTM than in CLIMATE SST are consistent with an increase in downward clear-sky radiation, which is the expected result for the RRTM code. Figure 1c indicates that the inclusion prognostic cloud water in the simulations PREDICTED CLOUD WATER and PCW+RRTM has a much larger impact than the inclusion of the RRTM code. The warmest CCM3 simulations are PREDICTED CLOUD WATER and PCW+RRTM. The surface temperature for these simulations are as much 10°C too warm during winter. Summer surface temperatures are less sensitive to the CCM3 parameterizations.

Figure 2 shows the 3-month average vertical temperature profiles for winter (June, July and August) and summer (December, January and February) at the South Pole. The observed profile for summer is from a composite of the 1961-2000 climatological values at standard levels (500, 300, 200, 150, 100 and 50 hPa), the 1957-2002 values at the surface, and 1988-1990 rawinsonde measurements from READER (Fig. 2b). From the rawinsondes, we gain a representation of the temperature profile in the lower troposphere. For winter, the strong inversion may not be well represented by the rawinsondes (Mahesh et al. 1997). Therefore, the surface and standard level temperature data for Fig. 2a are supplemented by Schwerdtfeger's (1984) temperature profile for the winter boundary layer. There are some differences in surface pressure for Fig. 2 due to representations of topography. The largest differences in temperature between the different model configurations are found in the lower troposphere. The standard version of CCM3 produces the coldest profiles in the lower troposphere. The RRTM simulation shows a slight warming, mostly in the lowest 50 hPa of the troposphere. The simulation PREDICTED CLOUD WATER shows a much larger warming in the lower troposphere. The warming is about 4°C during summer and 2°C during winter at the top of the inversion. The simulation with both PCW+RRTM is slightly colder at most levels, than PREDICTED CLOUD WATER, but the difference is almost always less than 2°C. The intensity of the winter inversion is well captured by the control simulation of CCM3, however, the height of the inversion is about 85 hPa above surface rather than about 50 hPa above surface for the observations. Other configurations of the NCAR climate model under-represent the inversion intensity. For example, the simulation PCW+RRTM has an inversion intensity about 9°C smaller than that of the observations. Furthermore, there are weak minima in the temperature profiles for CLIMATE SST and RRTM about 20 hPa above surface. The use of the prognostic cloud condensate eliminates these spurious minima, and the inversion heights above the surface for PREDICTED CLOUD WATER and PCW+RRTM are close to the observed value. The increase temperature lapse rate in the lower troposphere has consequences for the sensible heat flux that will be discussed in Section 6. The prognostic cloud condensate scheme, in addition to having more impact than the RRTM longwave radiation, results in some increased realism for the Antarctic temperature profile. All of the simulations exaggerate the sharpness of the lower-tropospheric temperature profile. The observations for winter, on the other hand, show a layer with a weak lapse rate between 525 hPa and 630 hPa above the boundary layer. There is a significant cold bias during summer at most levels for the CCM3 simulations. This bias is exceptionally large in the stratosphere where it can reach 20°C.

The summer temperature field is highly influenced by the surface albedo. Figure 3 shows the monthly surface albedo at the South Pole for April to September. Observed values are obtained from climatological radiation measurements provided by John King. The observed albedo over interior Antarctica does not display a large seasonal cycle unlike the Arctic case where summer melting can significantly reduce the reflection (e.g., Briegleb and Bromwich 1998a). South Pole values for CCM3 vary from 0.83 to 0.85 and are derived from the LSM linked with the atmospheric model. Observations suggest a value of about 0.81 during summer and slighter larger during spring and autumn when the sun is close to the horizon. The surface radiation balance during can be highly sensitive to the albedo over an ice surface as a change in albedo from just 0.80 to 0.81 results in a 5% reduction in

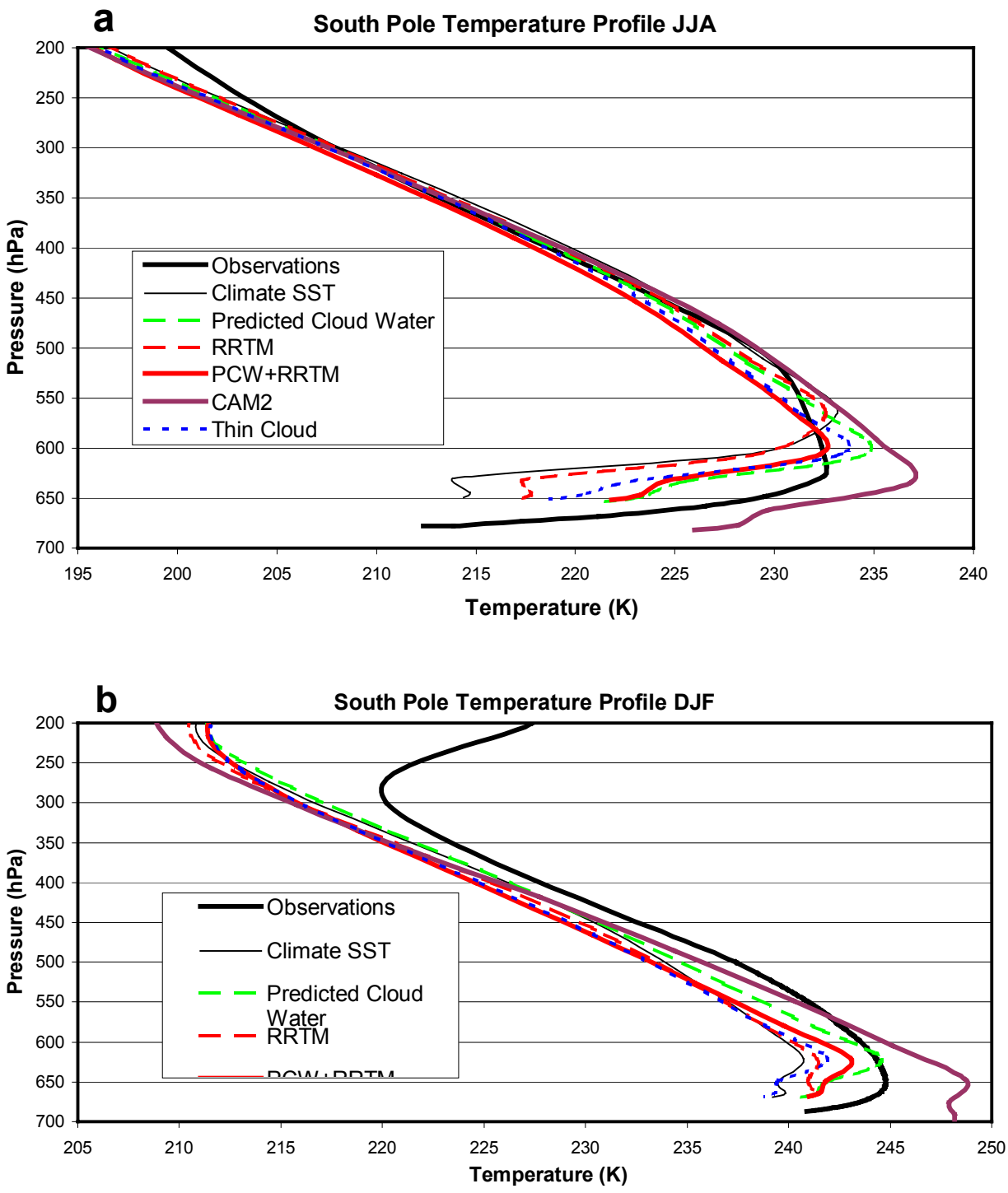

Figure 2. Vertical profiles of 3-month average temperature (K) from observations and model results at the South Pole for (a) winter and (b) summer. Observations are compiled from multi-year READER observations at standard pressure levels and the surface. Summer profiles are supplemented by 1988-1990 rawinsonde observations, and winter profile is supplemented by Schwerdtfeger (1984) boundary layer profile.

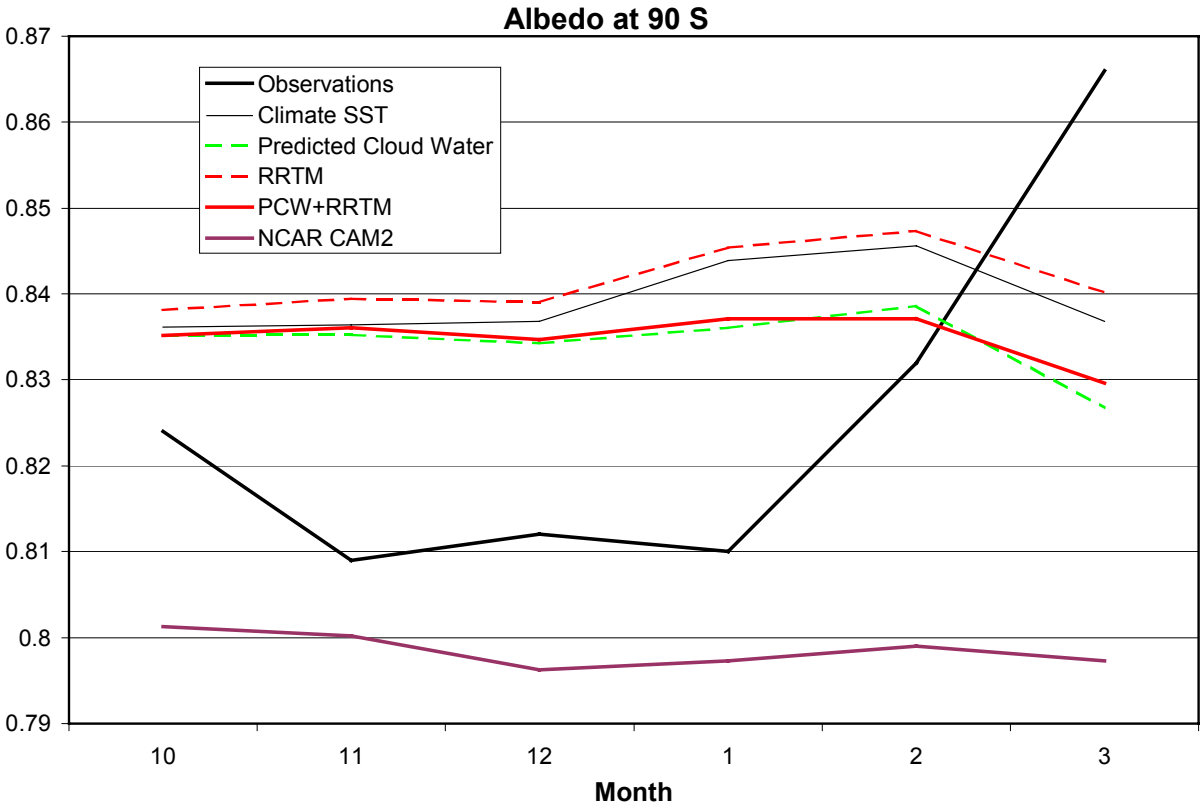

Figure 3. Monthly surface albedo at the South Pole.

absorbed shortwave radiation. Therefore, some of the summer cold bias in Figs. 1 and 2 for summer may result from a slightly large albedo. For CAM2, by contrast, the albedo is somewhat smaller, in the range 0.79-0.80. The reduction in Antarctic summer albedo for the Community Land Model with CCSM2 appears to be an important difference compared to that of LSM. The resulting increase in absorbed shortwave radiation contributes to the large warm bias during summer for the revised NCAR climate models (Figs. 1 and 2). In summary, Figs. 1-3 suggest that the best estimate of surface temperature for the Antarctic summer may be achieved with an albedo between that of CCM3 and CAM2.

4. ANTARCTIC CLOUDS

The observed cloud fraction over the South Pole is about 35% during winter and 55% during summer (Hahn et al. 1995). In contrast, the observed cloud fraction is about 75% along the Antarctic coast, as the cloud cover is large near the strong minimum in sea level pressure along the Antarctic circumpolar trough. The models CCM3 and CAM2 output cloud fraction based upon a diagnostic Slingo-type scheme. For the standard version of CCM3, this scheme is also used for the radiation calculations. The prognostic cloud condensate scheme is used to supply the longwave and shortwave radiative properties of clouds for CAM2 and those versions of CCM3 employing this scheme. Figure 4 shows the latitudinal distribution of CCM3 and CAM2 total cloud fraction for winter and summer over high southern latitudes. The CCM3 total cloud fraction over interior Antarctic is primarily from middle-level clouds, with the low-level clouds providing the largest contribution over the Southern Ocean. The difference is small for the diagnosed value of total cloud fraction between the different configurations of CCM3. During summer, total cloud fraction is large near the Antarctic coastline, in basic agreement with observations (Fig. 4b). Cloud fraction decreases south of 65°S in Fig. 4b. The values south of 85°S appear to be somewhat larger than the observed values from Hahn et al. (1995).

The diagnostic cloud fraction during winter has much less agreement with observations (Fig. 4a). Again, middle-level clouds dominate the contribution to total cloud fraction over interior Antarctica. The total cloud fraction is about 80% near the coastal latitudes, more or less reflecting the high observed cloud fractions there. The model cloud fraction, however, increases the south unlike the observed values. Near the South Pole, total cloud fraction is about 90%, perhaps more than twice the observed fraction. The Slingo-type scheme may work especially poor under the extremely cold conditions over the Antarctic Plateau pole as the saturation vapor pressure with respect to ice is extremely small thus the atmosphere is likely to be close to saturation or even supersaturated with respect to ice. Given the frequent occurrence of clear-sky precipitation at these latitudes, visible clouds can easily be absent even when the relative humidity is high (Bromwich 1988).

The diagnostic quantity known as effective cloud fraction provides useful insight on the radiative impact of the clouds. The effective cloud fraction is determined by multiplying emissivity by cloud fraction. Figure 5 shows the vertical distribution of effective cloud fraction for the polar cap south of 80°S. The standard version of CCM3 has effective cloud fraction heavily weighted towards the boundary layer, where the cloud fraction is very large. This is especially true during winter. There is some seasonal difference in the profiles, however, the overall cloud thickness does not show clearly larger values during either winter or summer. Rasch and Kristjansson (1998) find that, globally, the prognostic cloud scheme increases the height of the center of mass of cloud particles. This is also seen in Fig. 5 as the maximum is moved to more than 100 hPa above the surface for PREDICTED CLOUD WATER and PCW+RRTM. A significant amount of cloud condensate is located well above the maximum level for these simulations. The CCM3's vertical profile of effective cloud fraction appears to be qualitatively realistic with the use of the prognostic cloud scheme. It is less certain whether the vertical profile is quantitatively realistic. Figures 1 and 2 suggest the temperature field might be impacted by biases in the radiative effects of the clouds.

5. RADIATION

We now look at how the model parameterizations influence the radiation fields, especially at the earth's surface. Figure 6 shows the downward shortwave radiation and net (downward) shortwave radiation at the surface for the South Pole. Radiation observations are provided by John King. During December, the observed downward shortwave radiation is 442.7 W m^{-2} at the surface (Fig. 6a). The NCAR climate models produce smaller values by 30-45 W m^{-2}. The absorbed shortwave radiation at the surface is consistent with this difference, as the observed value is 83.1 W m^{-2} and the CCM3 values are 64-68 W m^{-2} during December (Fig. 6b). On the other hand, with a smaller albedo for CAM2, the absorbed shortwave is 81.5 W m^{-2}, very close to the observed value. Apparently, CCM3 clouds excessively block shortwave radiation from reaching the surface over Antarctica. The low albedo for CAM2 compensates for this.

Figure 7 shows downward longwave radiation and net (upward) longwave radiation at the surface. The positive net longwave radiation implies a longwave cooling at the surface. While, the shortwave radiation is zero during winter, the longwave radiation is important all year long. During winter months, surface cooling by the net longwave radiation lost into the atmosphere is primarily balanced by turbulent heat flux downward from the atmosphere. Latent heat flux and the heat storage rate in the ice are generally very small during winter. The surface energy balance is more complicated during

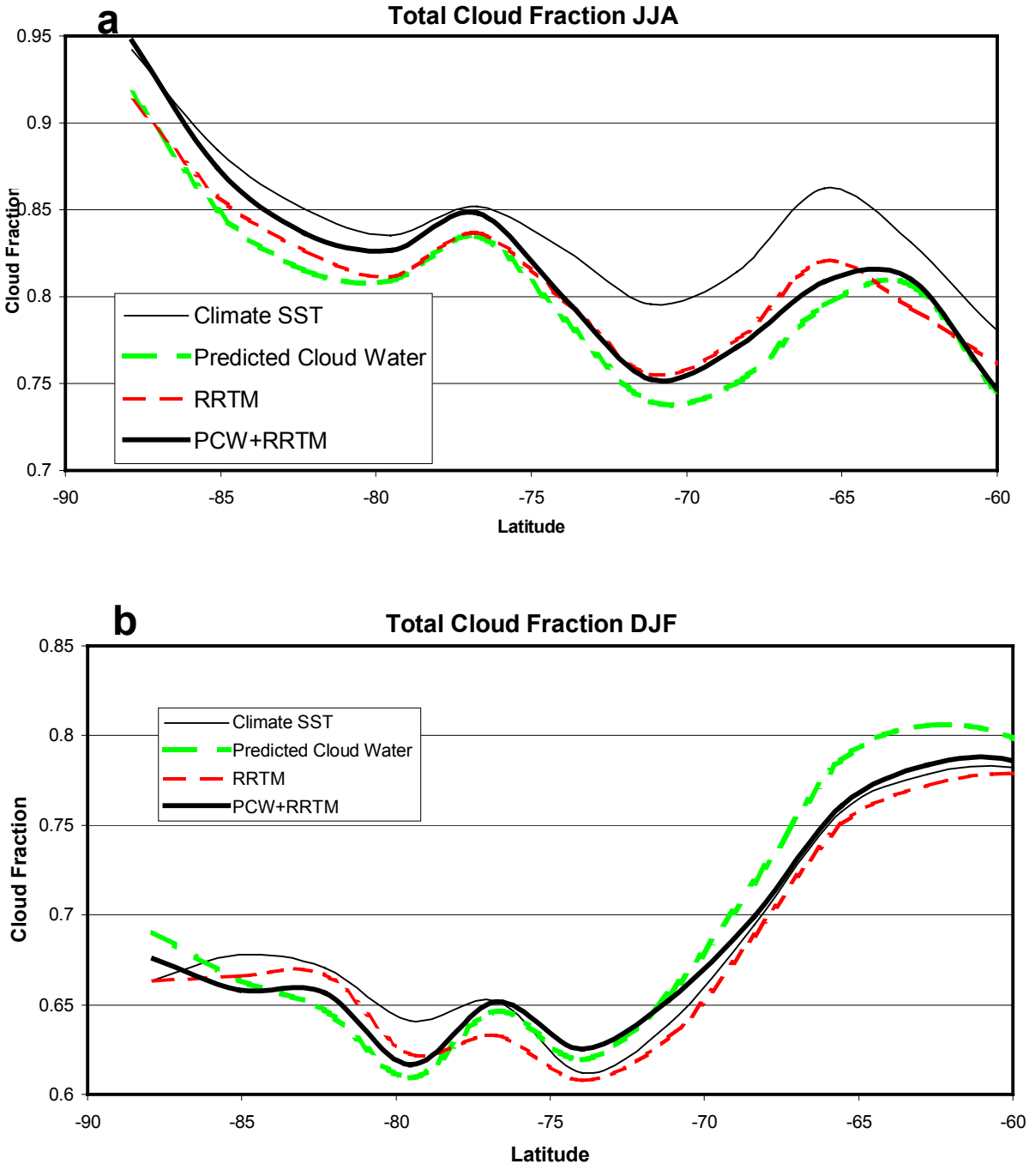

Figure 4. Three-month average total cloud fraction for (a) winter and (b) summer.

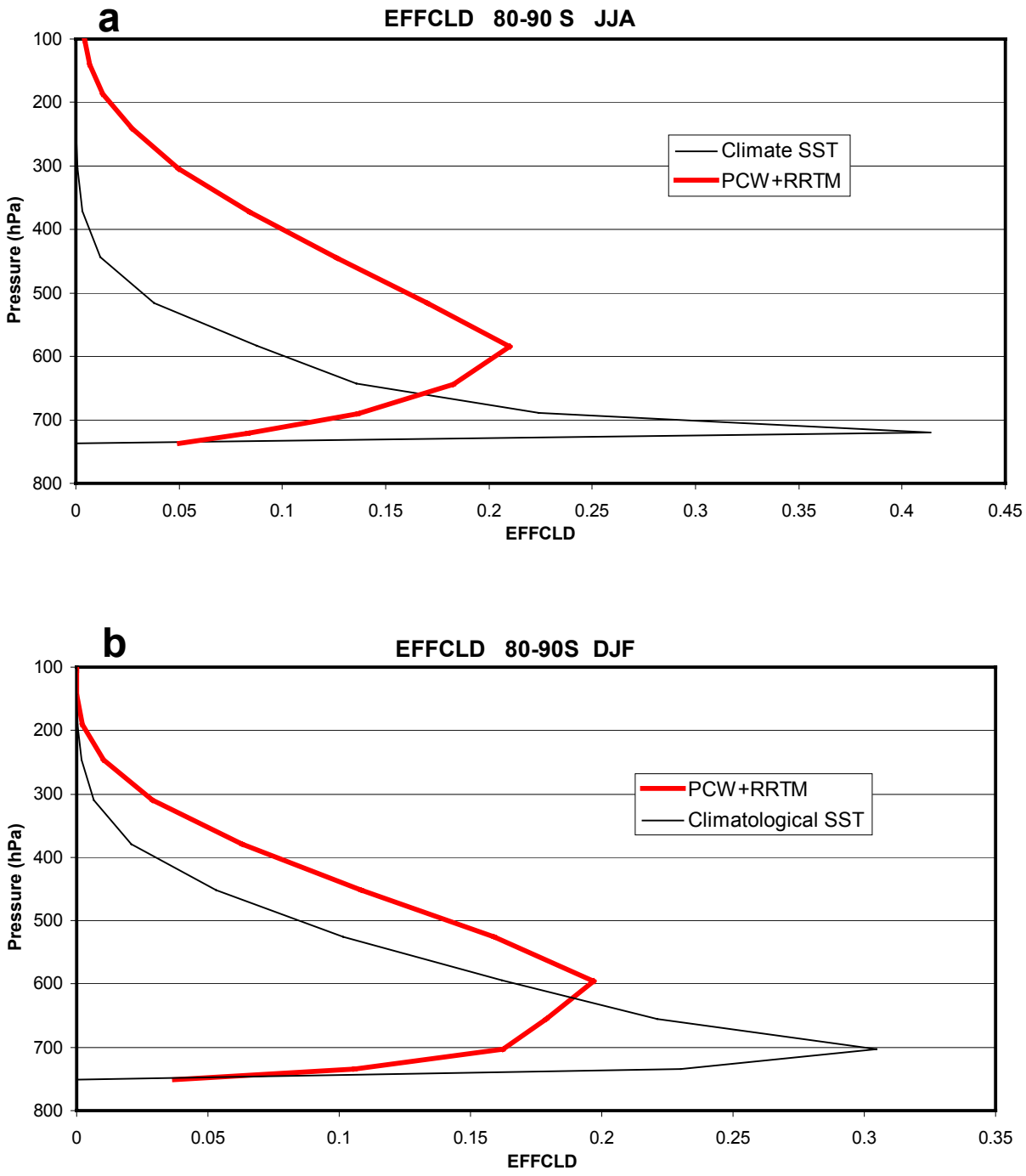

Figure 5. Vertical profiles of 3-month average effective cloud fraction for (a) winter and (b) summer.

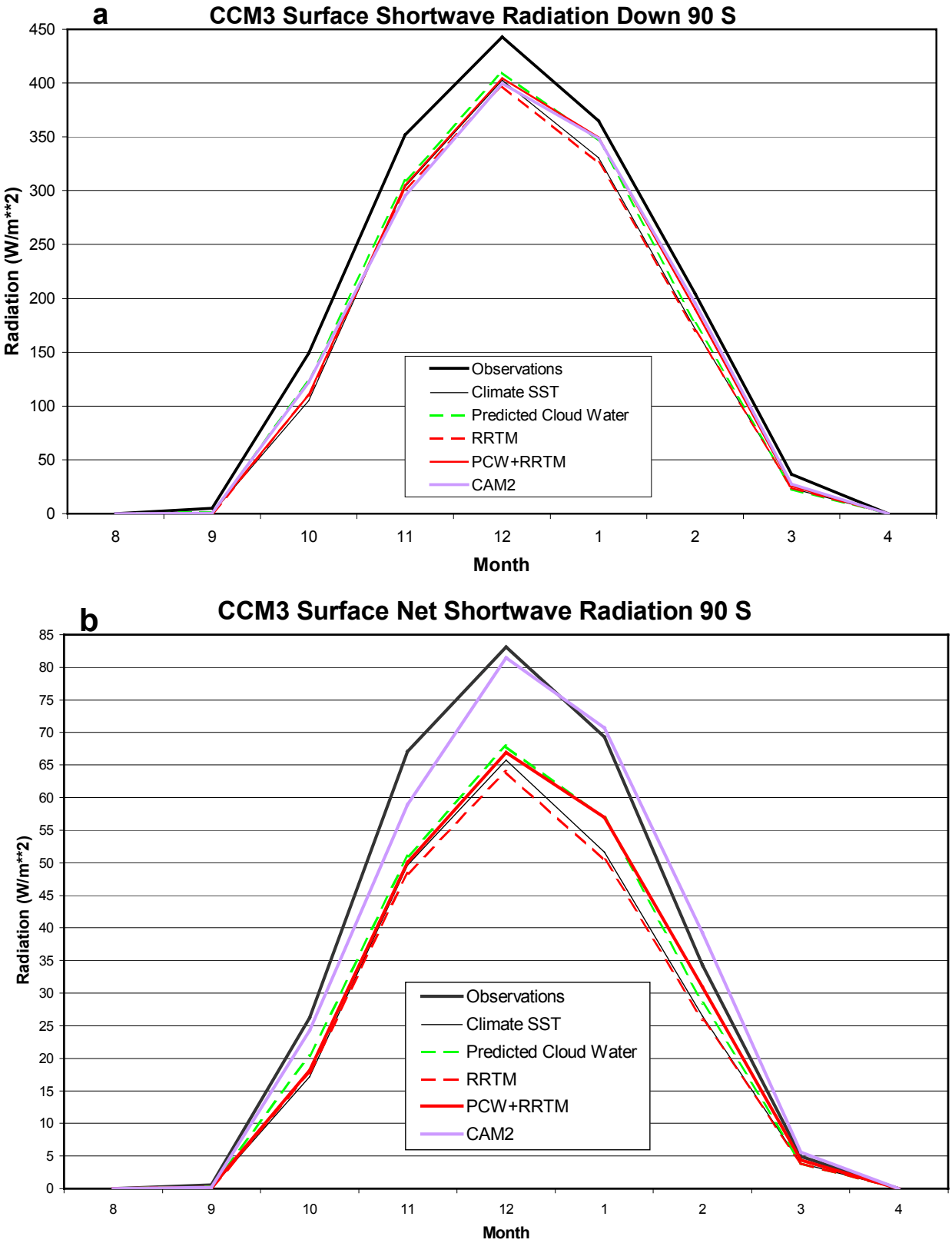

Figure 6. Monthly surface shortwave radiation (W $m^{-2)}$ at the South Pole for (a) the downward flux and (b) the net flux.

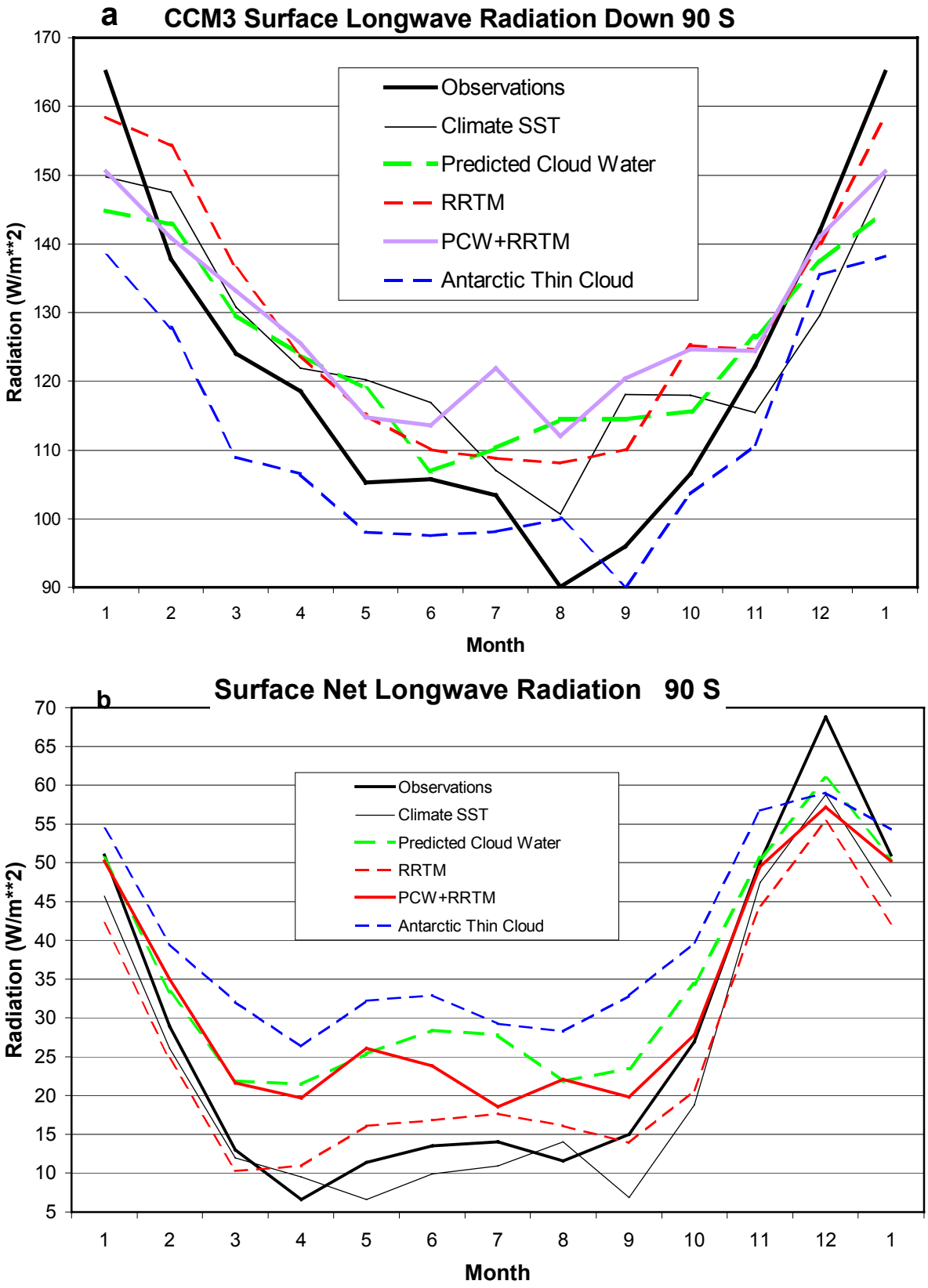

Figure 7. Monthly surface longwave radiation (W m^{-2}) at the South Pole for (a) the downward flux and (b) the net flux.

summer with shortwave heating and longwave cooling of the surface. Thus there is a tendency for the longwave and shortwave radiation to balance, with latent heat flux and sensible heat flux contributions also important. The net surface longwave radiation for the standard version of CCM3 is close to the observed value most of the year except for December when the longwave radiative cooling is too small by 10 W m^{-2}. The addition of prognostic clouds, however, to CCM3 in other simulations results in an increase in net longwave radiation. Again, the prognostic cloud condensate scheme has a larger impact than the RRTM.

The downward longwave flux in the CCM3 simulations is somewhat larger than the observed value most of the year. The observed annual average is 111.6 W m^{-2}, while the simulated values are 118.6, 119.1, 121.7, and 122.2 for the simulations CLIMATE SST, PREDICTED CLOUD WATER, RRTM and PCW+RRTM, respectively. The excess over the observed value is somewhat larger during winter, and the difference is smaller or even of the opposite sign during summer. All of these findings are consistent with significant cloud effects on the simulations. This is especially clear during winter in the absence of shortwave radiation. During summer, the cloud effects are more complicated as clouds can have a cooling effect by reflecting shortwave radiation and a warming effect by absorbing and emitting longwave radiation. The results shown in Fig. 7, together with excessive winter surface temperatures (Fig. 1) and insufficient incident shortwave radiation at the surface (Fig. 6) indicates excessive longwave and shortwave radiative impacts of the Antarctic clouds. Briegleb and Bromwich (1998a) note that the cloud water path for CCM3 was excessive by perhaps a factor of 2 in the polar regions, consistent with the results shown here.

6. CCM3 simulations with varied cloud thickness

In the climate model simulations using Kessler (1969) type cloud physics, autoconversion of cloud to precipitation is a key sink to atmospheric moisture substance. The parameterization of autoconversion of cloud ice to snow is much simpler in CAM2 than that of cloud liquid water to rain. As clouds over the Antarctic continent are largely composed of ice crystals, we examine the impact of changes to the ice autoconversion parameterization, which is parameterized as a simple mathematical expression,

$$\text{Autoconversion} = \text{Constant} \; (\; q_{ice} - q_{threshold} \;)$$

The cloud ice mixing ratio, q_{ice}, must exceed a specified threshold, $q_{threshold}$, for autoconversion to take place. The threshold is temperature sensitive and set at 5×10^{-6} for temperatures below -20°C, which commonly are found over interior Antarctica, even for the summer boundary layer.

There are few observations of ice cloud mass content over Antarctica that can be compared against the specifications for the autoconversion parameterization. Stone (1993) derived the ice content of clouds at the South Pole from radiation measurements. He expresses cloud thickness in terms of density. His values range from 0.3×10^{-6} to 6.0×10^{-6} kg m^{-3}. The autoconversion threshold for CCM3 is consistent with the upper end of Stone's observed range of ice cloud thickness, so the ice clouds must be relatively thick by Antarctic standards for autoconversion in CCM3. The newer model CAM2 also uses the same ice autoconversion parameterization. On the other hand, the presence of "clear-sky" precipitation (Bromwich 1988) without visible clouds suggests a low threshold is required for the initiation of precipitation over Antarctica. Thus, it is natural that we investigate the impact of a modified threshold for ice autoconversion. To test the sensitivity of Antarctic clouds to the threshold, a simulation referred to as **Thin Cloud** is performed with the cloud ice mixing ratio for autoconversion set at 1.0×10^{-6} kg per kg instead of 5×10^{-6} kg per kg. This new threshold value is representative of the middle of Stone's (1993) observed range. The new simulation is carried out for 15 years with the same boundary conditions as PCW+RRTM. Furthermore, a 5-year simulation referred to as **Thick Cloud** is performed with the threshold set at the increased value 10.0×10^{-6} kg per kg. Both of the new simulations have the RRTM longwave radiation scheme and prognostic clouds. Thus, they are directly comparable to PCW+RRTM.

The vertical distributions of effective cloud fraction for the new simulations are shown in Fig. 8. During winter, the effective cloud fraction is approximately twice as large in Thick Cloud than in Thin Cloud. The maximum value remains at the same level. During summer, there is only a slight change in cloud thickness in the boundary layer due to the threshold change. The effective cloud fraction, however, is significantly reduced in Thin Cloud above 600 hPa. As the cloud fractions (not shown) are similar for the simulations, the emissitivity differs by about a factor of 2 during winter, and somewhat less than that at most tropospheric levels during summer. Therefore, the simulations should be sensitive to the parameters of the simple ice autoconvesion parameterization. The Thin Cloud experiment may provide for an improved simulation of Antarctic climate, given the excessively thick radiative clouds have been thinned.

The results of the Thin Cloud experiment are included in Figs. 1, 2, 6, and 7. During winter, the surface temperature at the South Pole is about 5°C colder in the experiment with the reduced ice autoconversion threshold than for the simulation PCW+RRTM (Fig. 1a). The difference is largely confined to the boundary layer (Fig. 2). As the emissivity of the clouds is reduced, the downward longwave radiation for Thin Cloud is reduced by 10-20 W m^{-2} from the values for PCW+RRTM (Fig. 7a). Interestingly, the downward longwave flux for Thin Cloud is actually smaller than the observed at the

surface for all months except August. The small downward longwave flux is probably a consequence of the cold CCM3 tropospheres above the boundary layer (Fig. 2). While the reduced surface temperatures in Thin Cloud bring the upward longwave radiation closer to observations (not shown), the net longwave radiation field is not necessarily improved by the reduced autoconversion threshold for Thin Cloud. Fig. 8b shows that the net surface radiation is larger than the observed value by as much as 20 W m^{-2} during winter for this experiment. This excess over that observed is roughly double that for PCW+RRTM. The excess is manifested in increased emitted radiation from the warmer-than-observed surface during winter and insufficient downward radiation, especially during summer when the cold bias is most pronounced (Fig. 2b). The bias in net longwave radiation is balanced during winter by increased heat flux downward from the atmosphere. Sensible heat flux for the South Pole is shown in Fig. 9a. The thick solid line shows the estimated value from the Automatic Weather Station Patrick at 89.88°S for the year 1986 (Stearns and Weidner 1993). Climatological observations from the South Pole supplied by John King indicate a winter value of about -10 W m^{-2}, more or less in agreement with 1986 values for Patrick. The summer values for Patrick appear to be excessive, as the climatological values from John King indicate a combined sensible and latent heat flux of about 10 W m^{-2}. Figures 7b and 9a show that during winter there is an approximate balance between sensible heat flux and the net longwave radiation at the surface. During both summer and winter the sensible heat flux is negative (heat is transported downward from the atmosphere to the ice surface) for the NCAR models over interior Antarctica (Figs. 9b and 9c). The exception is the summer sensible heat flux for CAM2 that is slightly positive at some latitudes south of 80°S. Apparently, the warm bias connected with the lower surface albedo for CAM2 sometimes results in heat flux from the surface to the atmospheric boundary layer. Figure 9 also shows that the CCM3 heat flux from the atmosphere to the surface is larger for Thin Cloud than for other simulations. This is particularly true for winter when the zonal-average magnitude can exceed 30 W m^{-2}. The net longwave radiation has similar magnitude for the Thin Cloud experiment (Fig. 7b).

Thus, while the reduced autoconversion threshold for CCM3 ice clouds has reduced the longwave cloud emissitivity, which should be an improvement to the simulation, it has also exacerbated an improper surface energy balance in simulations with prognostic cloud water. This improper balance exists for the CCM3 simulations PREDICTED CLOUD WATER and Thin Cloud, as well as for CAM2 that also has the prognostic cloud scheme (Fig. 8b). The observed surface net longwave radiation is generally small, with a magnitude less than 15 W m^{-2} at the South Pole during winter. This is largely balanced by the sensible heat flux of similar magnitude, as the heat storage is generally smaller over climatological time scales. The small heat flux occurs in spite of the generally large vertical temperature gradient in the Antarctic boundary layer. The average magnitude of the observed inversion strength is about 20°C for the South Pole winter. Very high static stability suppresses heat transfer between the ice surface and the atmosphere. The detailed structure of the inversion, however, is often not well captured by numerical models with coarse vertical resolution of the shallow Antarctic boundary layer. King (1990) finds that surface similarity theory may not hold at heights above 5-10 m for the very stable boundary layer at Halley, Antarctica. Moreover, Cassano et al. (2001) note that if a model's vertical resolution does not capture the very stable surface layer then the downward sensible heat flux will probably be overestimated. As the lowest level for CCM3 is typically 50 m above the Antarctic plateau surface, excessive heat flux can be expected. In simulations of the standard version of CCM3, however, the sensible heat flux is somewhat suppressed by spurious temperature minima above the surface in the lower boundary layer as seen in Fig. 2a. With the inclusion of the prognostic cloud scheme, the temperature profiles in Fig. 2 are altered, more accurately reflecting the strong inverted lapse rate within the inversion. The smoother temperature profile, however, allows the increased heat flux seen in Fig. 9. Few current global climate models well resolve the very shallow surface boundary layer. Therefore, attention must be paid to the boundary layer problem to achieve an improved simulation of the Antarctic surface energy balance. Future efforts at modeling Antarctic clouds and radiation should address both the cloud radiative properties and the boundary layer.

7. CONCLUSIONS

Simulations with the NCAR CCM3 and the newest NCAR atmospheric climate model CAM2 are evaluated for their treatment of clouds and radiation over Antarctica. The present study expands upon the earlier work of Briegleb and Bromwich (1998a,b), which detailed the radiation budget and polar climate of CCM3. The parameterizations of clouds and radiation, the Rasch and Kristjansson (1992) prognostic cloud condensate scheme and the RRTM longwave radiative transfer algorithm have been included in a version of CCM3. The Rasch and Kristjansson scheme provides cloud optical properties that had been obtained from the diagnostic cloud scheme included within the standard version of CCM3. The RRTM alleviates the deficit in downward clear-sky longwave radiation (Mlawer et al. 1997; Briegleb and Bromwich 1998a). The Rasch and Kristjansson scheme is now the standard cloud scheme for CAM2. The RRTM is not included in CAM2. Nevertheless, the new longwave radiation parameterization for CAM2 is similar to RRTM in alleviating the clear-sky bias. Simulations with a standard version of CCM3 are compared to those with RRTM and the standard prognostic clouds, the standard longwave scheme and the prognostic cloud scheme,

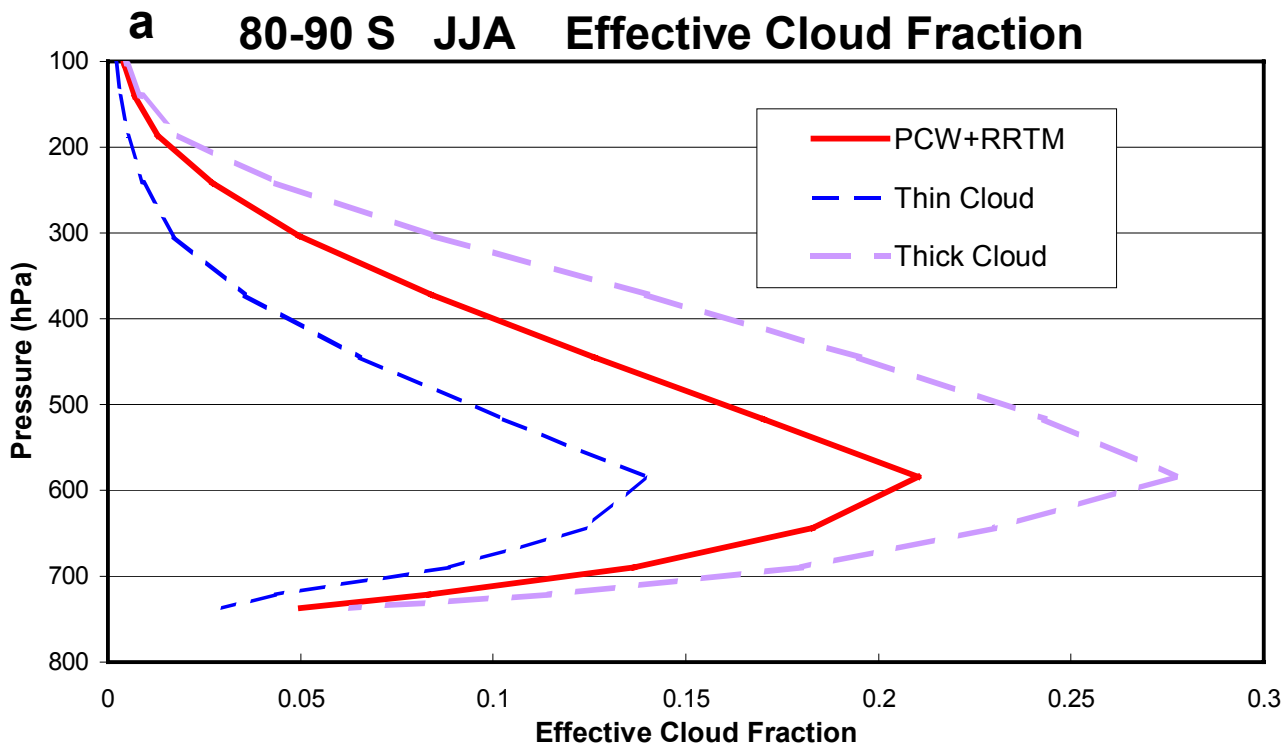

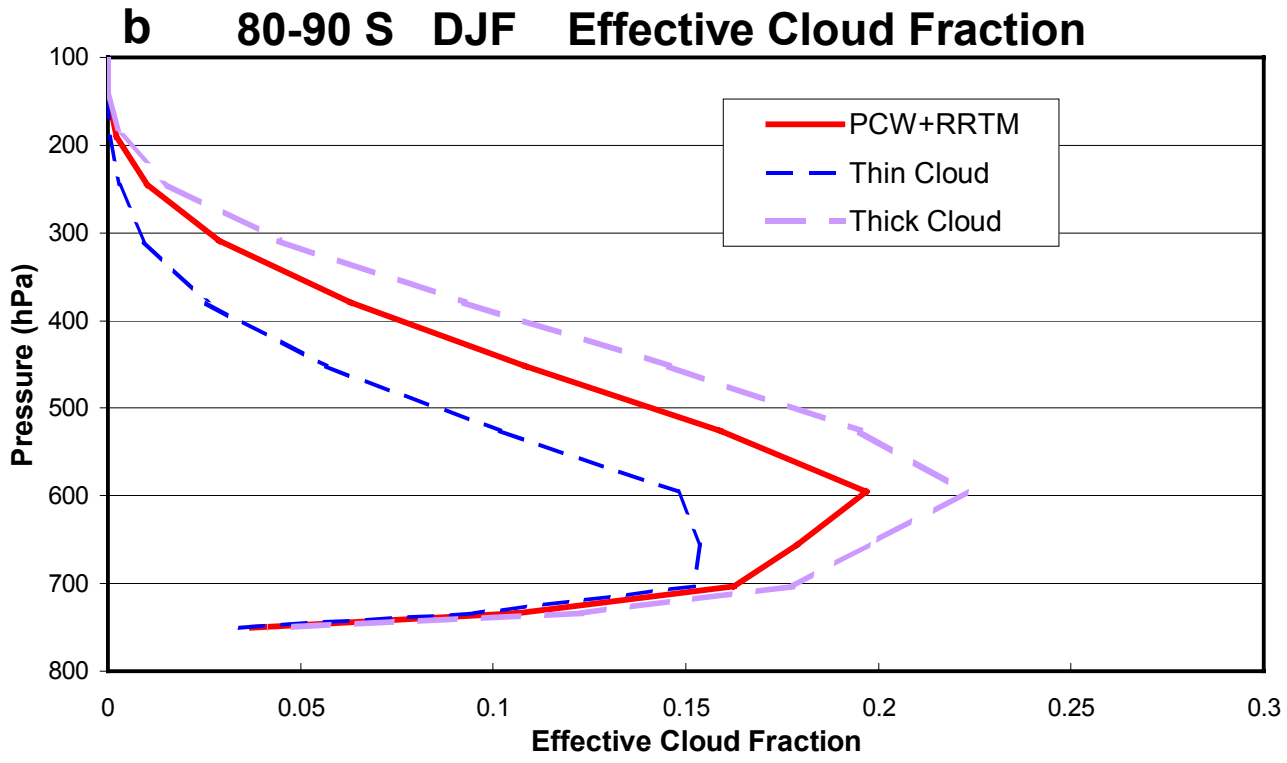

Figure 8. Vertical profiles of 3-month average effective cloud fraction for (a) winter and (b) summer.

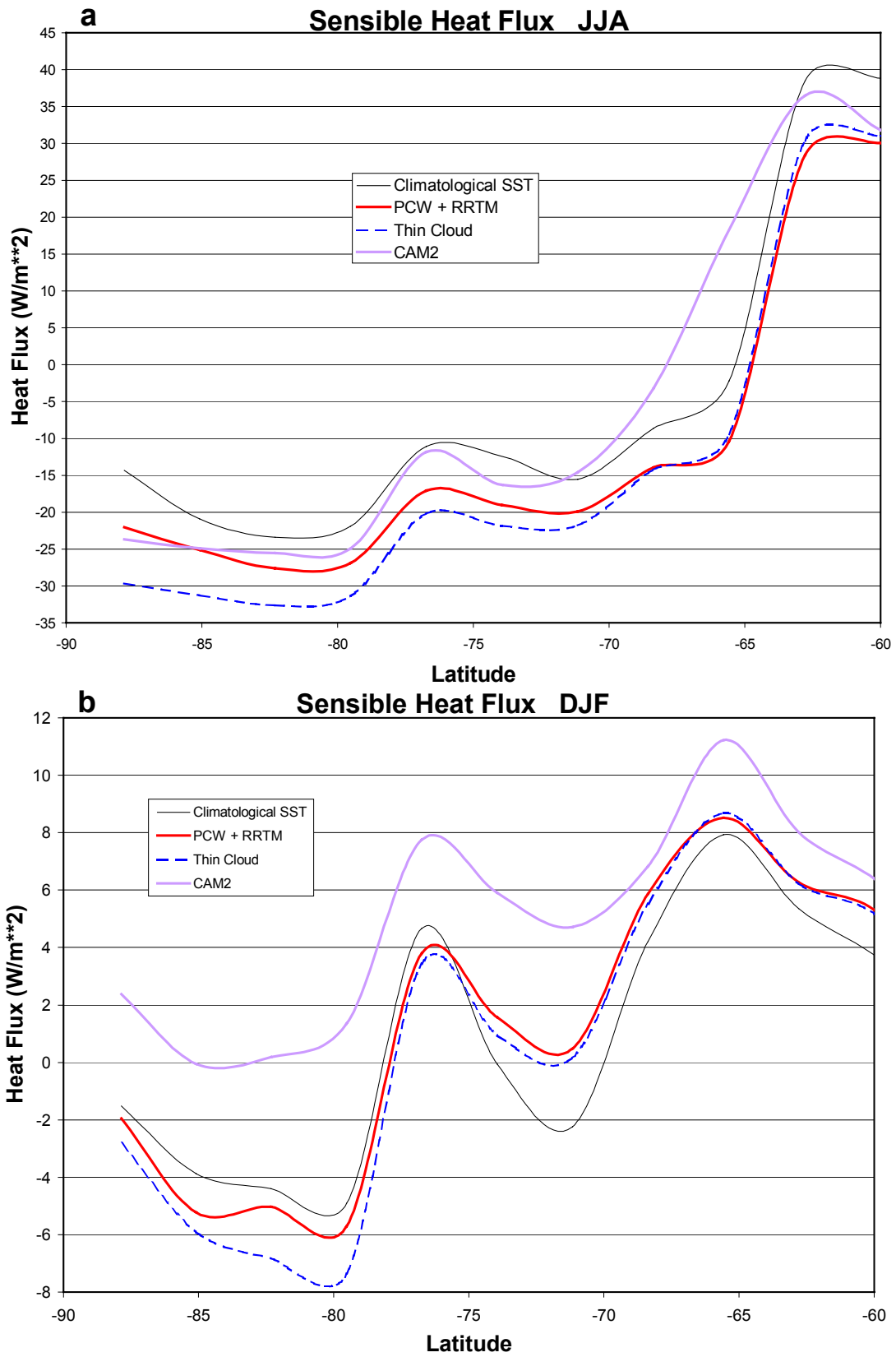

Figure 9. Sensible heat flux (W m^{-2}) shown for (a) monthly values at the South Pole, (b) three-month average for winter, and (c) three-month average for summer as a function of latitude.

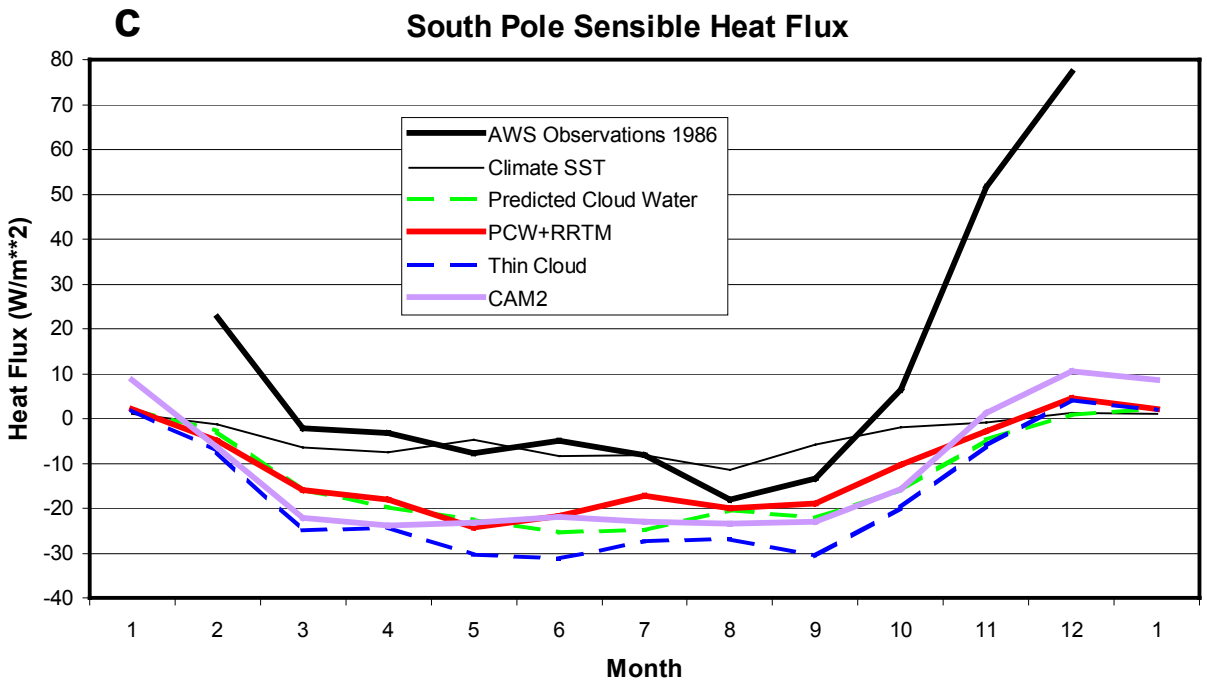

Figure 9. Sensible heat flux (W m^{-2}) shown for (a) monthly values at the South Pole, (b) three-month average for winter, and (c) three-month average for summer as a function of latitude.

and both RRTM and prognostic clouds. The simulations show a cold bias in the troposphere above the Antarctic boundary layer, especially during summer. The cold bias is as large as 20°C for the summer stratosphere.

The changes resulting from the introduction of prognostic clouds are much larger than those resulting from the introduction of RRTM. The prognostic cloud scheme results in increased cloud emissivity in the upper troposphere, reduced cloud emissivity in the lower troposphere, and an improved vertical distribution of cloud radiative properties over interior Antarctica compared to the simulation with a standard version of CCM3. Significant deficiencies are found in the simulation of Antarctic cloud radiative effects. The optical thickness of Antarctic clouds appears to be excessive, consistent with the findings of Briegleb and Bromwich (1998a). This results in a warm bias in surface temperature during winter and a deficit in downward shortwave radiation at the surface during summer. Several biases in the CCM3 simulations are larger with the prognostic cloud condensate scheme than with the standard diagnostic cloud scheme. The representations of Antarctic clouds and radiation by early versions of the new NCAR CAM2 are not clearly improved compared to those of the earlier CCM3. For example, the surface albedo over Antarctica is decreased in CAM2 and CCSM2 simulations in comparison to CCM3 simulations. This change contributes to a warm bias in tropospheric temperature during summer. Future versions of CAM2, however, are expected to include improvements resulting in a substantially modified polar radiation budget.

The simulations demonstrate the sensitivity of CCM3 to the mixing ratio threshold for autoconversion from suspended ice cloud to falling precipitation. In sensitivity simulations the threshold is given increased or decreased values. The emissivity of Antarctic clouds is found to be highly sensitive to the threshold, especially during winter. When the threshold is reduced towards a more realistic value, the Antarctic clouds are thinned and some of the biases in the temperature and radiation fields are reduced. However, the vertical resolution of the very shallow, very stable boundary layer is apparently insufficient to properly calculate the sensible heat flux. This leads to an improper winter balance between sensible heat flux and net longwave radiation at the surface. Both fields have excessive values. To improve the simulation of the surface energy balance, not only must the radiative effects of clouds be improved, it is also necessary to improve the boundary layer treatment.

.ACKNOWLEDGMENTS. This project is supported by National Science Foundation via grant NSF-ATM-9820042 and by NASA via grant NAG5-7750. The CCM3 simulations were performed with project 36091005 at NCAR, which is supported by NSF and grant PAS0689 from the Ohio Supercomputer Center, which is supported by the state of Ohio. The AVHRR and ISCCP data are obtained from the Cooperative Institute for Meteorological Satellite Studies at the University of Wisconsin-Madison. The automatic weather station data is obtained from the Antarctic Meteorological Research Center. James Rosinski of NCAR provided output from standard configuration simulations of the NCAR climate models.

8. REFERENCES

Anderson, P.S., 1993: Evidence for an Antarctic winter coastal polynya. *Antarct. Sci.*, **5,** 221-226.

Bonan, G.B., 1998: The land surface climatology of the NCAR Land Surface Model coupled to the NCAR Community Climate Model. *J. Climate*, **11,** 1307-1326.

Briegleb, B.P., and D.H. Bromwich, 1998a: Polar climate simulation of the NCAR CCM3. *J. Climate*, **11,** 1246-1269.

Briegleb, B.P., and D.H. Bromwich, 1998b: Polar radiation budgets of the NCAR CCM3. *J. Climate*, **11,** 1270-1286.

Bromwich, D.H., 1988: Snowfall in high southern latitudes. *Rev. Geophys.*, **26,** 149-168.

Cassano, J.J., T.R. Parish, and J.C. King, 2001: Evaluation of turbulent flux parameterizations for the stable surface layer over Halley, Antarctica. *Mon. Wea. Rev.*, **129,** 26-46.

Collins, W.D., 2001: Parameterization of generalized cloud overlap for radiative calculations in general circulation models. *J. Atmos. Sci.*, **58,** 3224-3242.

Collins, W.D., J.K. Hackney, and D.P. Edwards, 2002: An updated parameterization for infrared emission and absorption by water vapor in the National Center for Atmospheric Research Community Atmosphere Model. *J. Geophys. Res.*, **107,** in press.

Curry, J.A., W.B Curry, J.A., W.B. Rossow, D. Randall, and J.L. Schramm, 1996: Overview of Arctic cloud and radiation characteristics. *J. Climate*, **9,** 1731-1764.

Ebert, E.E., and J.A. Curry, 1992: A parameterization of ice cloud optical properties for climate models. *J. Geophys. Res.*, **97,** 3831-3836.

Gates, W.L., and Coauthors, 1996: Climate models - Evaluation. *Climate Change 1996,* J.T. Houghton, L.G. Meira Filho, B.A. Callander, N. Harris, A. Kattenberg, and K. Maskell, Eds., Cambridge University Press, 233-284.

Hahn, C., S. Warren, and J. London, 1995: Climatological data for clouds over the globe from surface observations, 1982-1991: Data tape documentation for the total cloud edition. *Numerical Data Package NDP-026A*, Available from Carbon Dioxide Information Analysis Center, Oak Ridge National Laboratory, Oak Ridge, Tenn.

Iacono, M.J., E.J. Mlawer, S.A. Clough, and J.-J. Morcrette, 2000: Impact of an improved longwave radiation model, RRTM, on the energy budget and thermodynamic properties of the NCAR Community

Climate Model, CCM3. *J. Geophys. Res.*, **105,** 14,873-14,890.

Kessler, E., 1969: On the distribution and continuity of water substance in atmospheric circulations. *Meteor. Monogr.* No. 32, **10,** Amer. Meteor. Soc., 84 pp.

Key, J., 2001: The Cloud and Surface Parameter Retrieval (CASPR) System for Polar AVHRR Data User's Guide. Space Science and Engineering Center, University of Wisconsin, Madison, WI, 62 pp.

Kiehl, J.T., J.J. Hack, G.B. Bonan, B.A. Boville, D.L. Williamson, and P. J. Rasch, 1998: The National Center for Atmospheric Research Community Climate Model: CCM3. *J. Climate*, **11,** 1131-1149.

King, J.C., 1990: Some measurements of turbulence over an Antarctic ice shelf. *Quart. J. Roy. Meteor. Soc.*, **116,** 379-400.

Lubin, D., and D.A. Harper, 1996: Cloud radiative properties over the South Pole from AVHRR infrared data. *J. Climate*, **9,** 3405-3418.

Lubin, D., B. Chen, D.H. Bromwich, R.C.J. Somerville, W.-H. Lee, and K.M. Hines, 1998: The impact of Antarctic cloud radiative properties on a GCM climate simulation. *J. Climate*, **11,** 447-462.

Mahesh, A., V.P. Walden, and S.G. Warren, 1997: Radiosonde temperature measurements in strong inversions: correction for thermal lag based on an experiment at South Pole. *J. Atmos. Oceanic Technol.*, **14,** 45-53.

Mlawer, E.J., S.J. Taubman, P.D. Brown, M.J. Iacono, and S.A. Clough, 1997: Radiative transfer for inhomogeneous atmospheres: RRTM, a validated correlated-k model for the longwave. *J. Geophys. Res.*, **102,** 16,663-16,682.

Morley, B.M., E.E. Uthe, and W. Viezee, 1989: Airborne lidar observations of clouds in the Antarctic troposphere. *Geophys. Res. Lett.*, **16,** 491-494.

Pinto, J.O. and J.A. Curry, 1997: Role of radiative transfer in the modeled mesoscale development of summertime arctic stratus. *J. Geophys. Res.*, **102,** 13,861-13,872.

Randall, D., J. Curry, D. Battisti, G. Flato, R. Grumbine, S. Hakkinen, D. Martinson, R. Preller, J. Walsh, and J. Weatherly, 1998: Status of and outlook for large-scale modeling of atmosphere-ice-ocean interactions in the Arctic. *Bull. Amer. Meteor. Soc.*, **79,** 197-219.

Rasch, P.J., and J.E. Kristjansson, 1998: A comparison of the CCM3 model climate using diagnosed and predicted condensate parameterizations. *J. Climate*, **11,** 1587-1614.

Schwerdtfeger, W., 1984: Weather and climate of the Antarctic. Elsevier, 261 pp.

Shibata, K., and M. Chiba, 1990: Effects of radiation scheme on the surface and wind regime over the Antarctic and on circumpolar lows. *NIPR Symp. Polar Meteor. Glaciol.*, **3,** 58-78.

Slingo, J.M., 1987: The development and verification of a cloud prediction scheme for the ECMWF model. *Quart. J. Roy. Meteorol. Soc.*, **113,** 899-927.

Slingo, A., 1989: GCM parameterization for the shortwave radiative properties of water clouds. *J. Atmos. Sci.*, **46,** 1419-1427.

Stearns, C.R., and G.A. Weidner, 1993: Sensible and latent heat flux estimates in Antarctica. *Antarctic Meteorology and Climatology: Studies Based on Automatic Weather Stations, Antarctic Research Series*, **61,** D.H. Bromwich and C.R. Stearns, Eds., American Geophysical Union, 109-138.

Stone, R.R., 1993: Properties of Austral winter clouds derived from radiometric profiles at the South Pole. *J. Geophys. Res.*, **98,** 12,961-12,971.

Tzeng, R.-Y., D.H. Bromwich, and T.R. Parish, 1993: Present-day Antarctic climatology of the NCAR Community Climate Model Version 1. *J. Climate*, **6,** 205-226.

Tzeng, R.-Y., D.H. Bromwich, T.R. Parish, and B. Chen, 1994: NCAR CCM2 simulation of the modern Antarctic climate. *J. Geophys. Res.*, **99,** 23,131-23,148..